



# Sound Pressure Kurtosis Analysis for Impact Pile Driving Including Noise Mitigation

Yaxi Peng, Ozkan Sertlek, and Apostolos Tsouvalas

## Contents

Introduction .....	2
SILENCE: Sound Source Modeling .....	3
SILENCE BUBBLE: Noise Mitigation Modeling .....	6
Kurtosis Analysis of Sounds from Offshore Pile Driving .....	7
Conclusions .....	9
References .....	10

## Abstract

Impact pile driving generates intense and impulsive underwater noise, which can have significant effects on marine life. As sound waves propagate away from the pile–water and pile–soil interfaces, their pressure characteristics evolve under the influence of seabed and sea surface reflections. Understanding these sound pressure waveform properties is essential for selecting appropriate metrics to assess noise impact on marine species, particularly in relation to established environmental noise thresholds. Commonly used exposure metrics, such as cumulative sound exposure level (SEL) and peak sound pressure level ( $L_{p, pk}$ ), provide important information but may not fully capture the complexity of noise impact across different species. Current impact assessments classify sound into only two mutually exclusive categories: impulsive and nonimpulsive. However, in reality, pulse length can vary with range and strike repetition rate. Given the impulsive nature of impact pile driving noise, this study investigates sound pressure kurtosis as a complementary metric to quantify the impulsiveness of

Y. Peng (✉) · A. Tsouvalas  
Delft University of Technology, Civil Engineering and Geoscience, Delft, The Netherlands  
e-mail: [y.peng@tudelft.nl](mailto:y.peng@tudelft.nl); [a.tsouvalas@tudelft.nl](mailto:a.tsouvalas@tudelft.nl)

O. Sertlek  
JASCO Applied Sciences Europe, Schwentinal, Germany  
e-mail: [ozkan.sertlek@jasco.com](mailto:ozkan.sertlek@jasco.com)

noise signals across various sediment types. Furthermore, the study models the application of a noise mitigation system, specifically an air-bubble curtain, to evaluate its effect on noise emission and subsequent changes in kurtosis. The findings provide insights into the variability of sound pressure kurtosis in both mitigated and unmitigated cases, offering a comprehensive understanding of the acoustic characteristics of impact pile driving noise and its potential effects on marine ecosystems.

---

### Keywords

Impact pile driving · Sound pressure kurtosis · Underwater noise · Noise impact assessment · Air-bubble curtain · Noise mitigation

---

## Introduction

The rapid expansion of offshore wind farms has raised significant concerns regarding their environmental impact on aquatic life. Although regulatory bodies have introduced strict underwater sound thresholds, evaluating these impacts remains challenging. To standardize the assessment of impact pile driving noise, dual exposure metrics are widely applied: cumulative sound exposure level (SEL) and peak sound pressure level ( $L_{p, pk}$ ). Exceeding either threshold can lead to auditory injury, increasing the risk of temporary threshold shift (TTS) or permanent threshold shift (PTS) in marine organisms. However, estimating the effects of anthropogenic noise across taxa such as fish, invertebrates, crustaceans, and marine mammals remains complex. Moreover, current impact assessment only classify sound into two mutually exclusive types: impulsive and nonimpulsive, even though in reality the pulse length can vary with propagation range, strike repetition rate, and many other factors.

Recent studies in humans and terrestrial mammals have shown that incorporating sound impulsiveness improves predictions of hearing loss risk (Hamernik and Qiu 2001). For marine species, kurtosis corrections have also been occasionally applied. For example, von Benda-Beckmann et al. (2022) demonstrated that kurtosis-corrected, frequency-weighted SEL accurately predicted the onset of low-level TTS in harbor porpoises. Further research has used kurtosis to characterize underwater sound from impulsive sources such as air guns, pile driving, and explosions (Müller et al. 2020; Guan et al. 2022). Sound pressure kurtosis, which depends on pulse shape and dispersion, varies with range and sediment type. The range variation of frequency-weighted kurtosis differs from the range variation unweighted kurtosis depending on the upper and lower limits of weighting functions for different marine animal groups (Sertlek et al. 2024).

Impulsive sounds from pile driving consist of repetitive sequences of broadband pulses that may act cumulatively on an animal's hearing. The magnitude of induced TTS is influenced by the total exposure duration, the interpulse interval between strikes, and the received SPL and spectrum. Controlled playback experiments with

harbor porpoises confirmed that pile driving noise can cause measurable TTS, and that the extent of auditory effects depends on both cumulative exposure and recovery during interpulse intervals.

To better capture the impulsive nature of such signals, kurtosis has been proposed as a quantitative metric of impulsiveness. For terrestrial mammals, a kurtosis value of 40 has been identified as the threshold separating nonimpulsive from fully impulsive sounds, and this criterion has been suggested as an initial reference point for marine mammals as well (Martin et al. 2020). A one-minute analysis window has been recommended for efficient computation and high accuracy in noise-induced hearing loss evaluation of human TTS (Tian et al. 2021). Furthermore, kurtosis-corrected, frequency-weighted SEL has been shown to improve predictions of TTS growth in harbor porpoises exposed to intermittent impulsive sounds (von Benda-Beckmann et al. 2022). These findings suggest that kurtosis can complement traditional exposure metrics, refining the assessment of noise impacts and bridging the gap between conventional dual criteria (SEL and  $L_{p, pk}$ ) and species-specific auditory effects. Nevertheless, it remains unknown how kurtosis varies during impact pile installation with and without noise mitigation systems, and how it changes with distance from the pile. The present study aims to investigate how kurtosis varies during impact pile installation with and without the application of a noise mitigation system.

---

## SILENCE: Sound Source Modeling

Over the past few decades, numerous computational models have been developed to predict underwater noise from offshore pile driving. Most approaches follow a two-step procedure: first, a detailed sound generation simulation, often based on finite element or finite difference methods (Reinhall and Dahl 2011), is used to capture the pile–water–soil interaction near the source; second, a sound propagation model projects the acoustic field to larger distances. Common propagation techniques include normal-mode analysis, wavenumber integration, and parabolic equation modeling (Lippert et al. 2016). More recently, the method of damped cylindrical spreading (DCS) and scaling laws have been developed, the latter allowing the dependence of sound exposure level on strike energy, pile diameter, water depth, and ram weight to be evaluated, including in cases with noise mitigation. In general, these methodologies have been extensively validated against SEL and  $L_{p, pk}$ , and their predictions are largely consistent. However, less attention has been devoted to temporal features of the sound pressure and to other metrics such as kurtosis, particle motion in the water, and ground vibrations in the upper sediment layer.

In this chapter, the SILENCE model is used to predict underwater noise radiation from offshore pile driving. As shown in Fig. 1, the complete SILENCE framework consists of two modules. First, a sound generation module simulates the interaction between the pile, the fluid, and the seabed, thereby capturing sound generation and propagation in the vicinity of the pile. Second, a sound propagation module, based on dynamic Green's functions and boundary integral equations (BIEs), is applied to

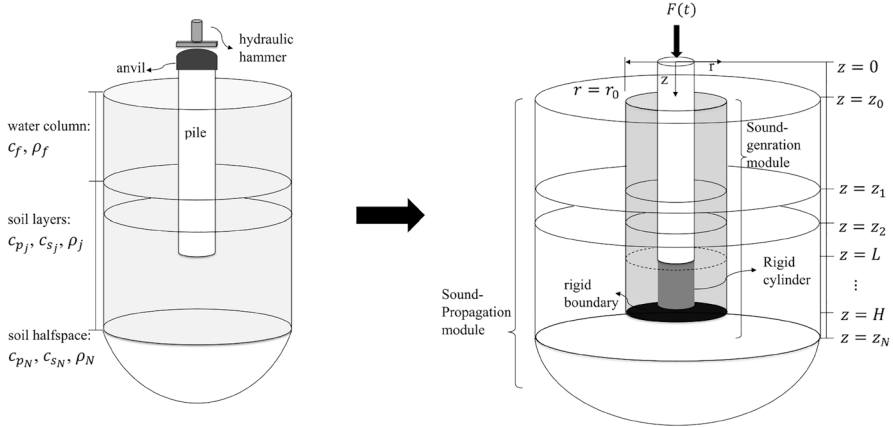


**Fig. 1** Schematic of the complete system (left) and the coupled SILENCE model (right). (Reproduced from Peng et al. (2021) © The Author(s), under CC BY license)

propagate the sound field to larger distances. This model improves computational efficiency and flexibility for predicting noise in both near- and far-fields. A detailed mathematical description of the SILENCE model is provided in Peng et al. (2021) and is omitted here for brevity.

The sound generation module is based on a three-dimensional cylindrically symmetric vibroacoustic model developed by Tsouvalas and Metrikine (2014). The module captures the dynamic interactions between the pile and the surrounding media. A modal decomposition is applied both to the shell structure and the acousto-elastic waveguide. Based on the mode-matching technique, the response of a coupled pile–water–soil system is obtained in the frequency domain. A set of the response functions in terms of pressure, velocity, displacement and stress tensors are obtained as input for the sound propagation model. The input to the sound propagation module is provided by the sound generation module through a boundary integral formulation. The direct boundary element method (BEM) is adopted to couple the sound generation and sound propagation modules. The solution of the acousto-elastic wavefield employs Somigliana’s identity in elastodynamics and Green’s third identity in potential theory (Peng et al. 2021). The velocity, displacement and pressure/stresses on the cylindrical boundary surface  $r = r_s$  are obtained from the sound generation module. The cylindrical surface in both the fluid and the soil domains need to be discretized when employing the direct BEM associated with the acousto-elastic layered half-space Green’s functions. The rule of thumb of using six elements per wavelength is adopted in the numerical integration of the line integral with the trapezoidal rule applied for the integration (Peng et al. 2021). In the fluid domain, the integration is based on the shortest wavelength of the compressional waves, while in the soil domain, the size of the element is governed by the shortest shear wavelength at the maximum frequency of interest. The model predictions are benchmarked against a theoretical scenario and validated using

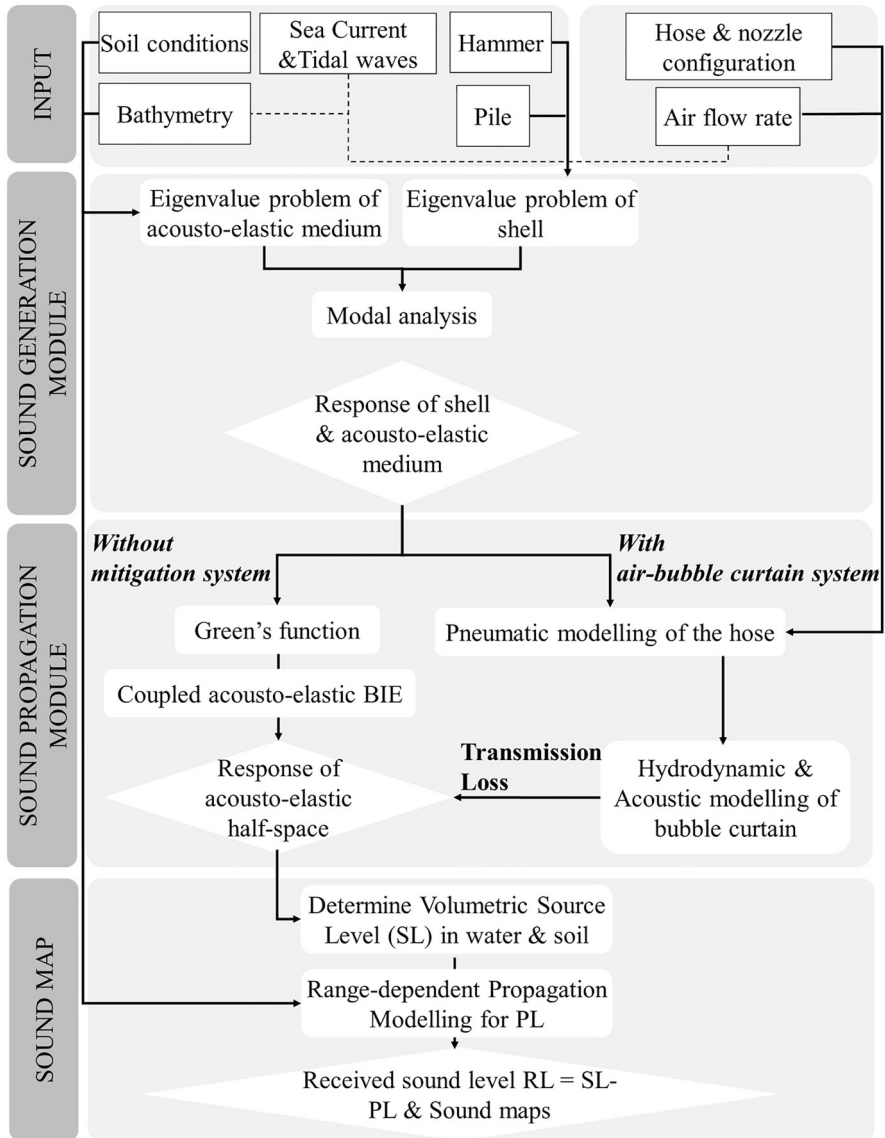


**Fig. 2** Diagram of the computational approach of SILENCE and SILENCE BUBBLE model and its components. (Reproduced from Peng, Y. (2025). © Yaxi Peng (2025). Used with permission/under terms of open access)

measurement data from a recent offshore pile-installation campaign as discussed in (Peng et al. 2021). The flow of the modeling activity is shown in Fig. 2.

## SILENCE BUBBLE: Noise Mitigation Modeling

Several noise mitigation systems (NMS) have been developed for offshore pile driving, ranging from source-based methods to shielding and resonator systems. Source mitigation, such as modified impact hammers and vibratory installation, reduces noise by altering pulse duration or shifting soil vibration modes. Shielding methods like noise mitigation screens and cofferdams decouple pile vibration from seawater, though their effectiveness decreases with larger monopiles and deeper water. Resonator-based systems and air-bubble curtains provide flexible, scalable solutions, but challenges remain in predicting performance, especially in complex seabed conditions and at lower frequencies. In this chapter, attention is focused on modeling the air-bubble curtain system, as it is among the most widely applied mitigation techniques in practice.

The air-bubble curtain system is usually modeled as a fully absorbing impedance boundary condition around the pile in the finite element models. A more physically realistic description was introduced by modeling the curtain as a homogeneous medium of constant thickness extending over the full water depth, with depth- and frequency-dependent wave speed. Building on this, Sertlek and Tsouvalas (2022) developed a coupled-mode theory model to describe wave propagation through a bubble curtain, exploiting the orthogonality of acousto-elastic modes. Bohne et al. (2020) improved the assumption of constant bubble distribution by introducing an integral approach to derive the local distribution of air fraction, enabling the calculation of an effective wavenumber that can be used in acoustic models to evaluate transmission characteristics of the curtain. The model incorporates the bubble formation process at the nozzle and coupled it to fluid dynamics, allowing bubble generation to be modeled at greater distances from the nozzle and providing a more realistic description of bubble distribution in operational systems.

Measurements of bubble curtains have examined hydraulic properties such as local void fraction and bubble size distribution. Hydrodynamic models (Bohne et al. 2020) highlight the need for accurate representation of the bubbly layer to capture its acoustic effect. Curtain performance can vary azimuthally due to uneven airflow through seabed pipes, while nozzle airflow rate strongly influences bubble generation and development. Soil conditions also play a critical role, as a significant portion of acoustic energy is transmitted through sediments.

It is worth noting that the existing models primarily focus on specific aspects of the modeling process related to pile driving noise when using the bubble curtain system, which highlight the need for a more comprehensive and unified modeling framework that accounts for all these critical factors.

To improve predictions of underwater noise from offshore pile driving, a three-dimensional multiphysics model is introduced for simulating air-bubble curtain systems (Peng et al. 2023). Figure 3 provides the overview of the complete system in SILENCE BUBBLE. The approach couples a hydrodynamic module describing bubble formation with a vibroacoustic boundary integral model for pile driving noise. Results show that accurately representing the acoustic properties of the bubbly layer is critical for reliable mitigation predictions. Bubble curtain performance can

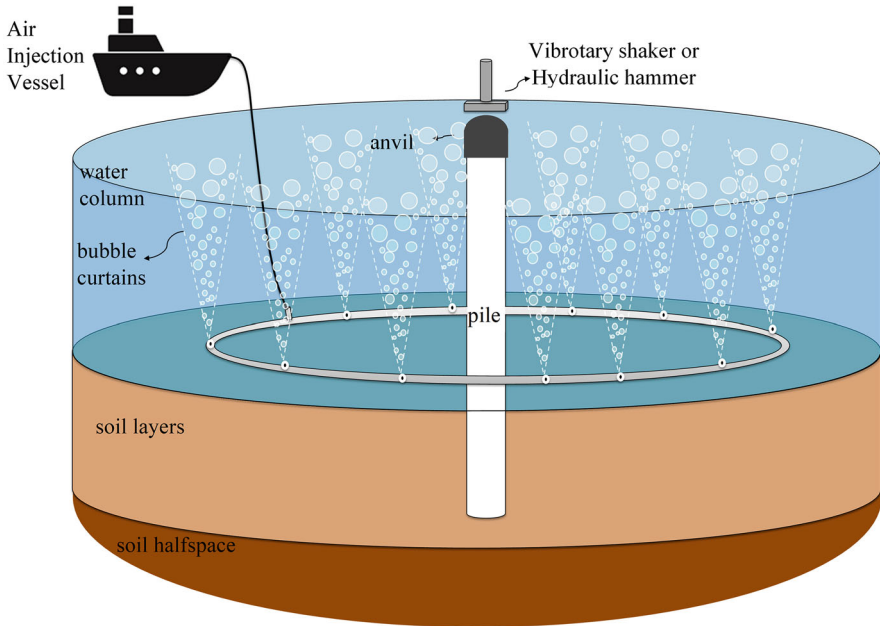


**Fig. 3** Overview of the complete system modeled in SILENCE BUBBLE

vary azimuthally due to uneven airflow through seabed pipes, making nozzle airflow velocity a key parameter for bubble generation and stability (Peng et al. 2023).

The complete framework integrates four modules: (i) a compressible flow model for air transport in perforated hoses, (ii) a hydrodynamic model for bubble cloud development across depth and range, (iii) an acoustic model for insertion loss of the curtain, and (iv) a vibroacoustic model of pile driving noise coupled to (iii) through a 3D boundary integral formulation. This model provides detailed outputs, including sound pressure, particle velocity, displacement, and stress within the sediment layers. Modeling particle motion in the water and the upper sediment layer is particularly important for assessing the impact of pile driving sounds on fish, as they are sensitive to both pressure and particle motion.

## Kurtosis Analysis of Sounds from Offshore Pile Driving

This study applies the kurtosis analysis methods proposed by Martin et al. (2020) and Müller et al. (2020) to the simulated dataset for an offshore pile installation campaign for both unmitigated pile and installation with the use of noise abatement system as a double air-bubble curtain system. The general statistical definition of kurtosis relates to the degree of heaviness in the tails of a statistical random variable or the distribution of sample values. In the context of a sound pressure time series, kurtosis follows the same definition, describing the distribution of pressure values.

It is independent of the temporal structure of the signal and the scaling of its amplitude. To resolve the ambiguity surrounding the term “impulsive signal” and to provide clearer characterizations, Müller et al. (2020) analyzed sound pressure field in time using kurtosis. The sound pressure kurtosis, denoted as  $\beta$ , is calculated as follows:

$$\beta = \frac{\mu_4}{\mu_2^2}$$

where  $\mu_4$  and  $\mu_2$  are the sound pressure variances defined as below:

$$\mu_4 = \frac{1}{t_1 - t_0} \int_{t_0}^{t_1} [p(t) - \bar{p}]^4$$

$$\mu_2 = \frac{1}{t_1 - t_0} \int_{t_0}^{t_1} [p(t) - \bar{p}]^2$$

where  $p(t)$  is sound pressure,  $\bar{p}$  is mean sound pressure, and  $t_0$  and  $t_1$  are the time points where the signal starts and ends, as described in ISO 18405:2017 (ISO 2017).

The model predictions are based on an offshore wind farm constructed in 2018. Table 1 summarizes the material and geometrical parameters, which were estimated from available geotechnical reports at the pile installation site. The forcing function was defined as a smoothed exponential impulse, corresponding to approximately 2000 kJ input energy into the pile. At this foundation location, the seabed consists of a thin marine sediment layer overlaying a stiff bottom-soil half-space. The configuration of the double big bubble curtain (DBBC) system is provided in Table 2.

The unmitigated sound field was predicted using the SILENCE model (Peng et al. 2021), while the mitigated case with an air-bubble curtain was simulated using SILENCE BUBBLE (Peng et al. 2023). Figure 4 presents the temporal evolution of sound pressure for both scenarios. From these time histories, sound pressure kurtosis was computed. Results show that kurtosis varies significantly when the air-bubble curtain is applied. Because kurtosis is not influenced by uniform amplitude scaling, the reduction in kurtosis indicates that the air-bubble curtain not only lowers

**Table 1** Basic input parameters for the simulations at the offshore wind farm in the German North sea

Parameter	Pile	Parameter	Fluid	Upper sediment	Bottom sediment
Length [m]	75	Depth [m]	40.1	1.5	$\infty$
Density [ $\text{kg}/\text{m}^3$ ]	7850	Density [ $\text{kg}/\text{m}^3$ ]	1000	1621.5	1937.74
Outer diameter [m]	8	$c_L$ [m/s]	1500	1603	1852
Wall thickness [mm]	90	$c_T$ [m/s]	–	82	362
The penetration depth [m]	30.5	$a_p$ [dB/ $\lambda$ ]	–	0.91	0.88
Maximum blow energy [kJ]	2150	$a_s$ [dB/ $\lambda$ ]	–	1.86	2.77

**Table 2** Basic input parameters for the air-bubble curtain system

Parameter	Air-bubble curtain
Location of the inner bubble curtain [m]	75
Location of the outer bubble curtain [m]	150
Nozzle diameter [mm]	1.5
Nozzle spacing [m]	0.3
Air flow rate [m <sup>3</sup> /min/m]	0.5

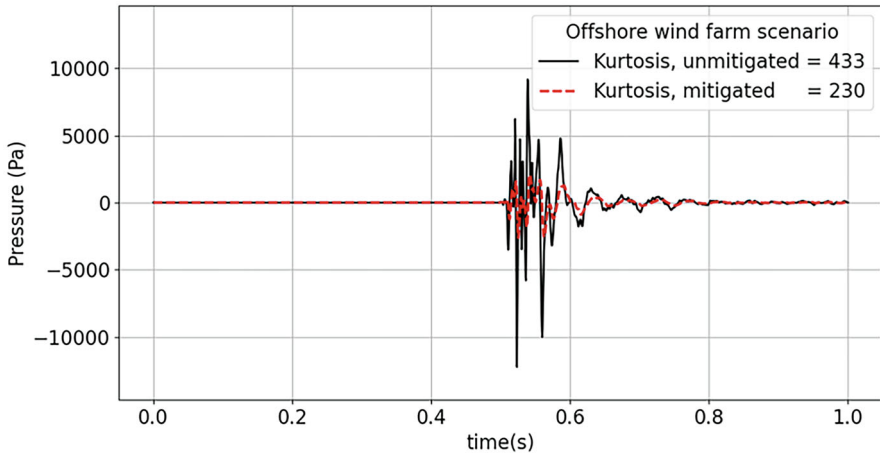


**Fig. 4** Computed time histories of the pressure and their Kurtosis in the water at 750 m horizontal distance from the pile and 2 m above the seabed with and without the noise mitigation system

the overall pressure level of the emitted noise but also alters the temporal distribution of the sound field.

This effect arises because the noise mitigation system blocks part of the direct transmission path through the water column, redirecting a considerable fraction of the acoustic energy into the sediment layer. The transmission loss of the NMS is frequency dependent, in this analysis, the mitigation of the DBBC system is more efficient at higher frequencies. As a result, different wavefronts and waveform shapes emerge in the mitigated field compared to the unmitigated case. The values presented here correspond to single-strike signals; however, kurtosis can vary across different ranges and may also depend on integration time and strike repetition rate when sequences of impulses are analyzed.

## Conclusions

In this chapter, the study demonstrates that sound pressure kurtosis offers valuable complementary information to conventional underwater noise metrics such as cumulative SEL and peak sound pressure level, particularly for characterizing the pulse length of impact pile driving noise. The results show that kurtosis is sensitive

to the application of noise mitigation systems and provides additional insight into waveform shape changes that occur during propagation. Modeling of an air-bubble curtain reveals not only a reduction in overall sound levels but also a notable decrease in kurtosis, indicating a less impulsive noise signature in the mitigated field. These findings highlight the potential of integrating kurtosis into noise impact assessments, thereby improving the evaluation of species-specific risks and the effectiveness of mitigation measures. Incorporating such waveform-based metrics into regulatory frameworks could lead to more ecologically relevant and targeted underwater noise management strategies. It remains to be investigated whether predictions of kurtosis metrics are consistent with field measurements. Further studies are needed to determine how kurtosis values, when combined with frequency weighting functions and compared against established thresholds, relate to auditory impacts in marine species and to assess their applicability in environmental impact assessments.

**Competing Interest Declaration** The author(s) has no competing interests to declare that are relevant to the content of this manuscript.

---

## References

- Bohne T, Griebmann T, Rolfes R (2020) Development of an efficient buoyant jet integral model of a bubble plume coupled with a population dynamics model for bubble breakup and coalescence to predict the transmission loss of a bubble curtain. *Int J Multiphase Flow* 132:103436. <https://doi.org/10.1016/j.ijmultiphaseflow.2020.103436>
- Guan S, Brookens T, Miner R (2022) Kurtosis analysis of sounds from down-the-hole pile installation and the implications for marine mammal auditory impairment. *JASA Express Lett* 2(7):071201. <https://doi.org/10.1121/10.0012348>
- Hamernik RP, Qiu W (2001) Energy-independent factors influencing noise-induced hearing loss in the chinchilla model. *J Acoust Soc Am* 110(6):3163–3168. <https://doi.org/10.1121/1.1414708>
- ISO (2017) ISO 18405:2017 underwater acoustics—terminology. International Organization for Standardization, Geneva
- Lippert S, Nijhof M, Lippert T, Wilkes D, Gavrilov A, Heitmann K, Ruhnau M, von Estorff O, Schäfer A, Schäfer I (2016) COMPILER—a generic benchmark case for predictions of marine pile-driving noise. *IEEE J Ocean Eng* 41(4):1061–1071. <https://doi.org/10.1109/JOE.2016.2524738>
- Martin SB, von Lucke K, Barclay DR (2020) Techniques for distinguishing between impulsive and non-impulsive sound in the context of regulating sound exposure for marine mammals. *J Acoust Soc Am* 147(4):2159–2176. <https://doi.org/10.1121/10.0000971>
- Müller RAJ, von Benda-Beckmann AM, Halvorsen MB, Ainslie MA (2020) Application of kurtosis to underwater sound. *J Acoust Soc Am* 148:780–792. <https://doi.org/10.1121/10.0001631>
- Peng Y (2025) Underwater sound propagation and mitigation in offshore pile driving. Doctoral thesis, Delft University of Technology, Delft. <https://doi.org/10.4233/uuid:61f71fd9-1b7f-4bd0-b47b-e6c43abdf279>
- Peng Y, Tsouvalas A, Stampoultzoglou T, Metrikine A (2021) A fast computational model for near- and far-field noise prediction due to offshore pile driving. *J Acoust Soc Am* 149(3):1772–1790. <https://doi.org/10.1121/10.0003752>

- Peng Y, Laguna AJ, Tsouvalas A (2023) A multi-physics approach for modelling noise mitigation using an air-bubble curtain in impact pile driving. *Front Mar Sci* 10:1134776. <https://doi.org/10.3389/fmars.2023.1134776>
- Reinhall PG, Dahl PH (2011) Underwater Mach-wave radiation from impact pile driving: theory and observation. *J Acoust Soc Am* 130(3):1209–1216. <https://doi.org/10.1121/1.3614540>
- Sertlek HO, Tsouvalas A (2022) Underwater sound propagation through an air-bubble medium in an acousto-elastic waveguide. In: *Proceedings of the 28th international congress on sound and vibration (ICSV28)*, Singapore, 24–28 July 2022
- Sertlek HO, Peng Y, Ainslie MA, von Benda-Beckmann AM, Halvorsen MB, Koessler MW, Küsel ET, MacGillivray AO, Tsouvalas A (2024) Effects of sediment properties, distance from source, and frequency weighting on sound pressure and sound pressure kurtosis for marine airgun signatures. *J Acoust Soc Am* 156(6):4242–4255. <https://doi.org/10.1121/10.0034709>
- Tian Y, Ding W, Zhang M, Zhou T, Li J, Qiu W (2021) Analysis of correlation between window duration for kurtosis computation and accuracy of noise-induced hearing loss prediction. *J Acoust Soc Am* 149(4):2367–2376. <https://doi.org/10.1121/10.0003954>
- Tsouvalas A, Metrikine A (2014) A three-dimensional vibroacoustic model for the prediction of underwater noise from offshore pile driving. *J Sound Vib* 333(8):2283–2311. <https://doi.org/10.1016/j.jsv.2013.11.045>
- von Benda-Beckmann AM, Ketten DR, Lam FPA, de Jong CAF, Müller RAJ, Kastelein RA (2022) Evaluation of kurtosis-corrected sound exposure level as a metric for predicting onset of hearing threshold shifts in harbor porpoises (*Phocoena phocoena*). *J Acoust Soc Am* 152(1):295–301. <https://doi.org/10.1121/10.0012364>

**Open Access** This chapter is licensed under the terms of the Creative Commons Attribution-NonCommercial-NoDerivatives 4.0 International License (<http://creativecommons.org/licenses/by-nc-nd/4.0/>), which permits any noncommercial use, sharing, distribution and reproduction in any medium or format, as long as you give appropriate credit to the original author(s) and the source, provide a link to the Creative Commons license and indicate if you modified the licensed material. You do not have permission under this license to share adapted material derived from this chapter or parts of it.

The images or other third party material in this chapter are included in the chapter's Creative Commons license, unless indicated otherwise in a credit line to the material. If material is not included in the chapter's Creative Commons license and your intended use is not permitted by statutory regulation or exceeds the permitted use, you will need to obtain permission directly from the copyright holder.

